

Dynamics of Relaxation Phenomena in Spherical Tokamak

T. Hayashi, N. Mizuguchi, H. Miura, and T. Sato
National Institute for Fusion Science (NIFS), Toki, Japan
e-mail contact of main author: Hayashi@nifs.ac.jp

Abstract. Three-dimensional magnetohydrodynamic (MHD) simulations are executed to clarify the physical mechanisms of MHD relaxation activities, specifically the Internal Reconnection Event (IRE), which are observed in the spherical tokamak experiments. For a case of an initial equilibrium with $q(0)$ less than one, tunnel-like plasma jet flow is formed by the occurrence of the external magnetic reconnection accompanying the growth of localized deformation of torus. When initial $q(0)$ is slightly greater than one, upon increase of beta, multiple mode number of finer-scale ballooning type instabilities is triggered, where the typical toroidal mode number n is 11. In the nonlinear stage, the surface of the torus is deformed due to growth of those medium- n modes, and a part of heat energy is lost into the external region through occurrence of external reconnection. Interestingly, low n modes, particularly $n=2$, are enhanced presumably by nonlinear coupling among the unstable medium- n modes, and the $n=2$ type deformation of the torus becomes dominant in the later stage.

1. Introduction

The spherical tokamak has revealed itself several favorable properties such as compactness and excellent stability in high-beta plasmas. As the progress of experiments, it has been shown that several unique features are observed in the dynamical processes of spherical tokamak plasmas. A phenomenon that is often called Internal Reconnection Event (IRE) is one of such feature, which has been generally observed in the spherical tokamak experiments such as START [1] and NSTX [2], and is considered to be an energy relaxation phenomenon. We have been executing three-dimensional magnetohydrodynamic (MHD) simulations to investigate the physical mechanisms of the event.

In the previous papers [3,4], the simulation started from an initial axisymmetric equilibrium that had been chosen rather arbitrarily. We mainly studied a case for which the central value of the safety factor, $q(0)$, was slightly less than one for the initial equilibrium. The simulation results were compared with experiments, and were shown to reproduce a couple of key features of IRE observed in the thermal quench phase of START. In those simulations, simultaneous excitation of multiple low n pressure-driven (interchange type) modes around the $q=1$ surface and a spontaneous phase-alignment among the dominant modes were observed. Because of this nature, expansive bulge-like deformation grew on the surface of the torus. Consequently, an external magnetic reconnection, which occurs between the field lines in the torus and external fields was induced. The external reconnection caused convective loss of the plasma heat energy through formation of plasma jet flow due to the pressure imbalance along the reconnected field lines.

In this paper, in Section 3, we point out findings that a tunnel-like structure of plasma jet flow is formed inside the torus when external reconnection occurs, which causes quick expulsion of heat energy stored inside the torus. Moreover, in Section 4, results for a new series of simulation runs are shown, where the initial condition is given by a numerically reconstructed equilibrium of the NSTX experiment obtained just before an occurrence of IRE, for which $q(0)$ is slightly greater than one.

2. Simulation Modeling

We execute magnetohydrodynamic simulations in a toroidal geometry. The boundaries of the computation region are assumed to be a perfect conducting wall. The governing equations consist of the full set of resistive and compressible magnetohydrodynamic equations as follows:

$$\frac{\partial \rho}{\partial t} = -\nabla \cdot (\rho \mathbf{v}), \quad (1)$$

$$\frac{\partial}{\partial t}(\rho \mathbf{v}) = -\nabla \cdot (\rho \mathbf{v} \mathbf{v}) - \nabla p + \mathbf{j} \times \mathbf{B} + \mu(\nabla^2 \mathbf{v} + \frac{1}{3}\nabla(\nabla \cdot \mathbf{v})), \quad (2)$$

$$\frac{\partial \mathbf{B}}{\partial t} = -\nabla \times \mathbf{E}, \quad (3)$$

$$\frac{\partial p}{\partial t} = -\nabla \cdot (p \mathbf{v}) - (\gamma - 1)p \nabla \cdot \mathbf{v} + (\gamma - 1)(\eta \mathbf{j}^2 + \Phi), \quad (4)$$

$$\mathbf{j} = \nabla \times \mathbf{B}, \quad (5)$$

$$\mathbf{E} = -\mathbf{v} \times \mathbf{B} + \eta \mathbf{j}, \quad (6)$$

$$\Phi = 2\mu(e_{ij}e_{ij} - \frac{1}{3}(\nabla \cdot \mathbf{v})^2), \quad (7)$$

$$e_{ij} = \frac{1}{2}(\frac{\partial v_i}{\partial x_j} + \frac{\partial v_j}{\partial x_i}). \quad (8)$$

A finite difference scheme having fourth-order accuracy both in time and space is utilized. The numerical grid consists of, typically, 128x64x128 and 74x64x180 points.

3. Simulation Results for $q(0) < 1$

The details of the simulation results for an initial equilibrium with $q(0) < 1$ were described in the previous paper [4]. Here we point out the structure of the plasma jet flow that is formed by the occurrence of the external magnetic reconnection accompanying the growth of localized deformation. Shown in Fig. 1 (a) are the three-dimensional structures of the plasma pressure (iso-surface), the vector field of a pair of the plasma jet flows (fine arrows) and the magnetic field lines (thick lines). The plasma flows consist of a pair of convections with the opposite toroidal component to each other, and are almost parallel to the field lines. Those lines passing the localized deformation are emerging from the internal region and are connected to the external region. The pressures on them are definitely higher than those on other field lines that exist entirely on the external region. It implies that the plasma pressure actually flows out of the torus along the reconnected field lines. It is seen that two bunches of the flow are formed toward the top and the bottom of the torus originated from the inside of the torus. Interestingly, as is shown in Fig.1 (b) plotted for only the one side of the pair flow, it is possible to go against the jet flows up to the deep inside the torus, since the flows have a simple tunnel-like structure

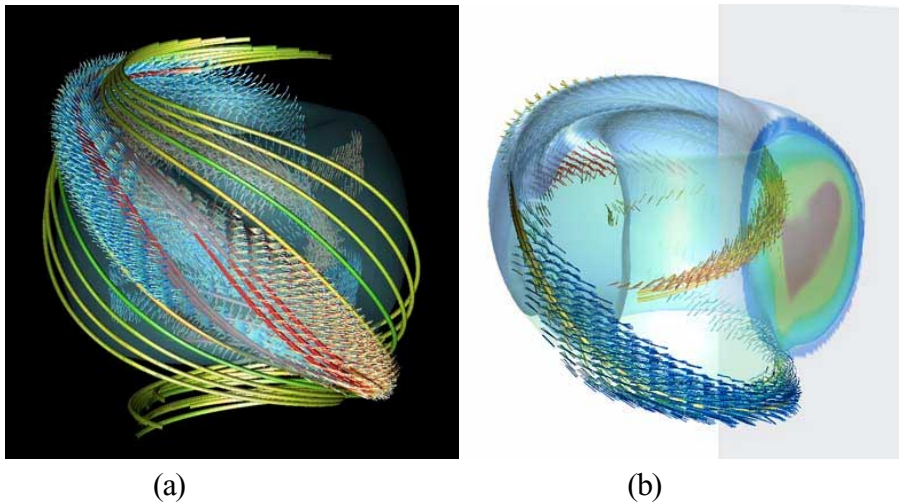


Fig.1 (a) Three-dimensional structure of plasma pressure, flow (vector arrows) and magnetic field lines in the simulation result, when a pair of the jet flow is formed along the externally reconnected field lines. (b) Similar plot as (a), but only the one side of the pair flow (vector arrows) is shown to see formation of the structure of the tunnel-like jet flow inside the torus. Shown on the poloidal cross section is the pressure profile.

inside the torus. It is observed that the core hot plasma region is directly connected to the external cold plasma region by the tunnel-like flow. The heat energy stored inside the torus is ejected in this mechanism, much like to put a hole on a rubber ball. It should be pointed out that the basic structure of the torus is not disrupted even at this highly deformed stage. The outflow of pressure ceases when about 40 % of the heat energy is lost. The resultant deformations in the overall shape of the plasma are in good agreement with the experimental observations.

4. Simulation Results for $q(0) > 1$

For the simulation runs described in this section, as is shown in Fig.2, the initial condition is given by the EFIT equilibrium code, which has been adjusted to reconstruct equilibria of the NSTX experiment [5] (The data was provided by courtesy of Drs. S.A. Sabbagh and S.M. Kaye). The boundary shape of the computation region is adjusted to follow roughly the device geometry, by using a modified version of the simulation code that incorporates non-uniform grid interval scheme. The initial equilibrium indicates that $q(0)$ is 1.14, the aspect ratio A is 1.29, the elongation is 1.7, the triangularity is 0.44, and the central beta value is 4.3%. The simulation code, as well as the linearized version of the code, indicates that this configuration is stable. In the simulation, the plasma pressure gradually increases because of the Ohmic heating of the plasma current. Onset of unstable modes is observed when the central beta arrives at around 20%.

Shown in Fig. 3 is the time evolution of each Fourier component of the magnetic energy (the $n=0$ component is not plotted). Multiple numbers of unstable modes, which have the nature of the medium- n ballooning instabilities, are excited, where the typical toroidal mode number n is 11. The structure of the $n=11$ mode is plotted in Fig.4 (a), which indicates that the mode grows mainly in the outside boundary region. In the nonlinear stage, the shape of the torus surface is deformed due to the growth of the modes, as is plotted in Fig.4 (b). The external reconnection is induced by the deformation of the surface, although the deformation has a finer structure compared with the case of $q(0) < 1$ shown in Section 3. Thus the heat energy is lost into the external region by formation of convective flow along the reconnected field lines.

A noticeable feature observed in the plot of Fig.3 is the trigger of low n modes, in particular $n=2$, which are initially stable but are excited suddenly at around $t=100-120$. One possible explanation of the delayed onset of those low n modes is that nonlinear coupling produces them among the medium- n modes, such as $n=10, 11, 12,$ and 13 . Another interesting feature of Fig.3

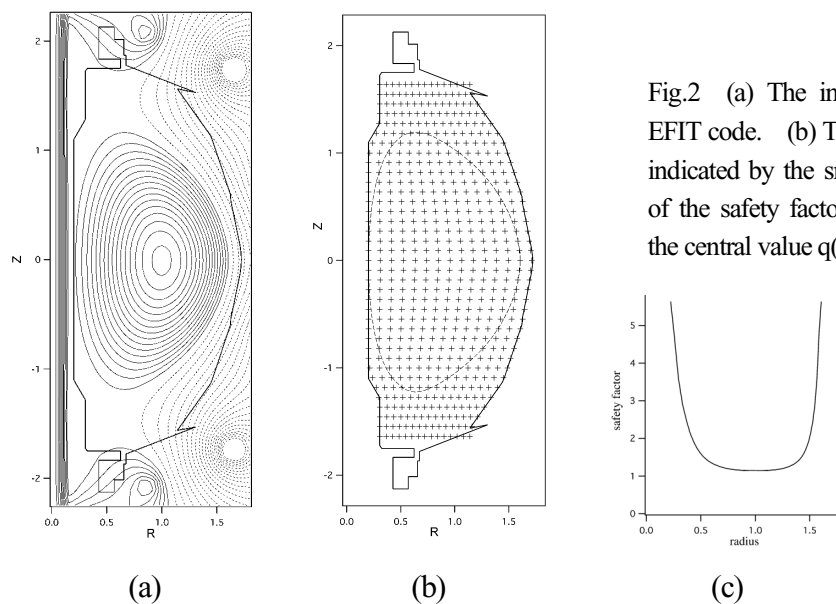


Fig.2 (a) The initial equilibrium computed by the EFIT code. (b) The shape of the simulation region is indicated by the small + marks. (c) The initial profile of the safety factor q versus the major radius, where the central value $q(0)$ is 1.14.

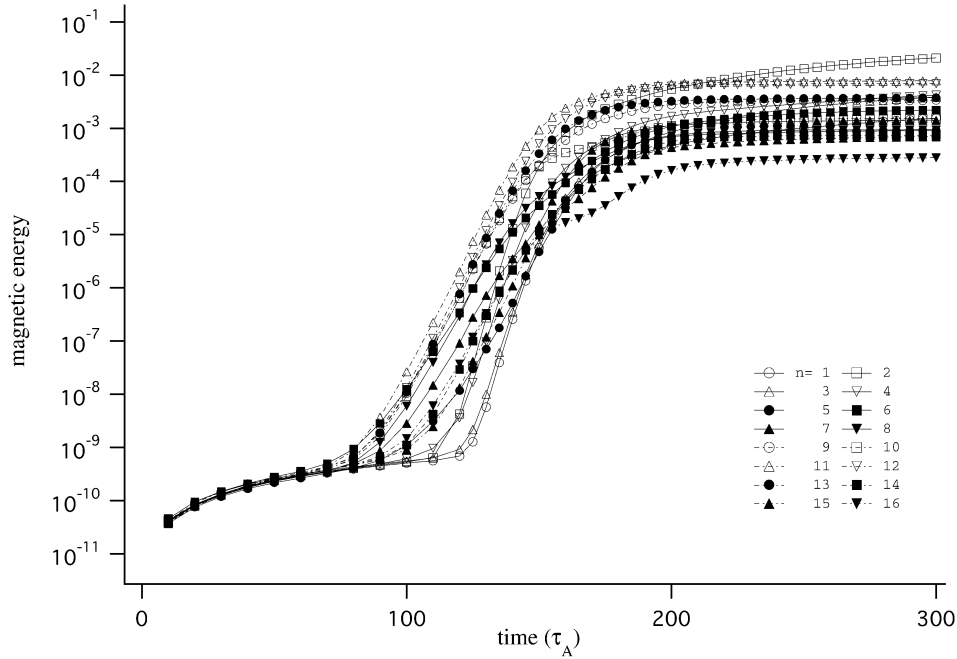


Fig.3 Growth of perturbation in the magnetic energy for each toroidal Fourier mode n

is that the $n=2$ mode continues to grow even after activities of other modes including the $n=11$ mode are saturated at around $t=170$. It should be noted, as is shown in Fig.5, that the total kinetic energy excited by the unstable modes sharply grows between $t=150$ and 170 , has a peak value at around $t=170$, but quickly decays between $t=170$ and 250 . The fine structure of deformation of the torus surface, as is shown in Fig. 4 (b), is gradually smoothed out, and is replaced by the smoother $n=2$ structure. In the later stage, at $t=300$, the $n=2$ mode becomes dominant. The overall shape of the torus at $t=300$ is shown in Fig. 5 by a plot of iso-surface of the plasma pressure.

5. Discussion

The plasma convective flow induced by the external magnetic reconnection is formed for both cases of $q(0) < 1$ and $q(0) > 1$, which are described in this paper. The flow speed, however, is much faster for the $q(0) < 1$ case because in this case the plasma core region is directly connected with the external region by the reconnected field lines. Thus, significant pressure imbalance appears along the reconnected field lines. On the other hand, for the $q(0) > 1$ case, the unstable medium- n modes grow mainly in the boundary region, and only the boundary region is connected with the external region by

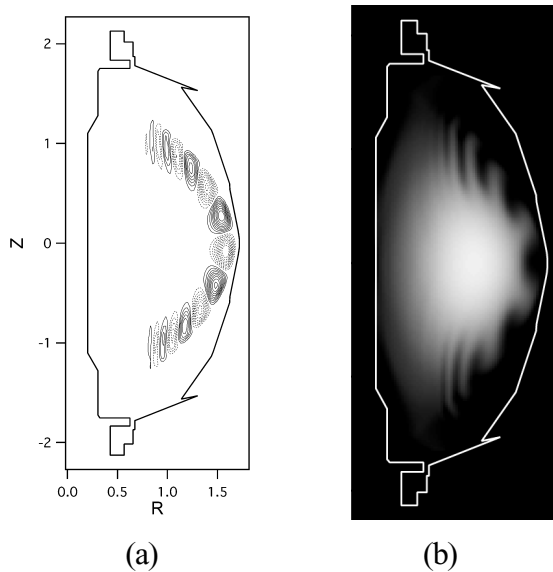


Fig.4 (a) The mode structure of the $n=11$ mode at $t=120$ (τ_A). (b) Deformation in the plasma pressure profile in a poloidal cross-section due to the nonlinear growth of the modes at $t=150$ (τ_A).

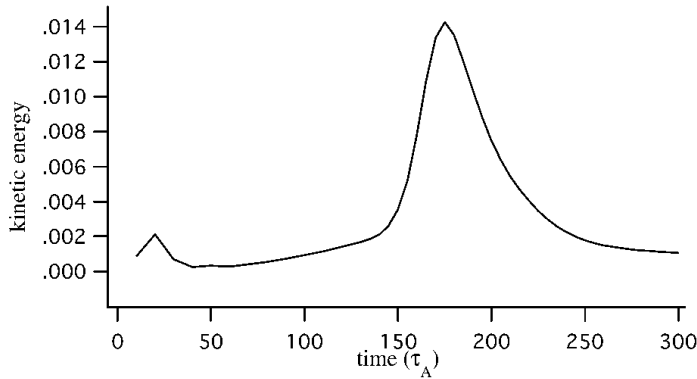


Fig.5 Time evolution of the total kinetic energy

the reconnected field lines, while clear nested surfaces remain in the core region.

In both cases, the unnecessary part of the heat energy is expelled to the ambient region without destroying the whole torus while keeping the favorable property of the resiliency. It seems that the spherical tokamak can efficiently readjust its own profile without destroying the whole torus owing to the existence of such mechanism. The relaxation to the state with the $n=2$ deformation observed in the $q(0)>1$ case can possibly suggest a transition to a relaxed state that is governed by some general rule.

In the previous paper [4], we observed two-step relaxation, where $q(0)$ is initially less than one but becomes greater than one after the first step relaxation. In this case, excitation of an $m=2/n=1$ resistive current-driven mode was observed as the second step for a relatively higher resistive situation, which has more or less disruptive nature. In this paper in Section 4, the simulation starts from $q(0)>1$ equilibrium, but the $m=2/n=1$ mode is not visible. This might suggest subtleness of profile dependency of the process.

Acknowledgements

The authors would like to express their thanks to the NSTX experimental group, especially Drs. S.A. Sabbagh and S.M. Kaye for providing them with the EFIT equilibrium data. Drs. M. Gryaznevich and A. Sykes are acknowledged for valuable discussions on experimental observations of START and MAST. Numerical computations were performed at the Advanced Computing System for Complexity Simulation of National Institute for Fusion Science.

References

- [1] Sykes A., Phys. Plasmas 4 (1997) 1665.
- [2] Kaye, S.M., et al, in Proceedings of the 27th EPS Conference, Budapest, 2000, P4-046.
- [3] Hayashi T., Mizuguchi N., Watanabe T., Todo Y., Sato T., Nuclear Fusion, 40 (2000) 721.
- [4] Mizuguchi N., Hayashi T., and Sato T., Phys. Plasmas, 7 (2000) 940.
- [5] Sabbagh, S.A., et al, in Proceedings of the 27th EPS Conference, Budapest, 2000, P1-043.

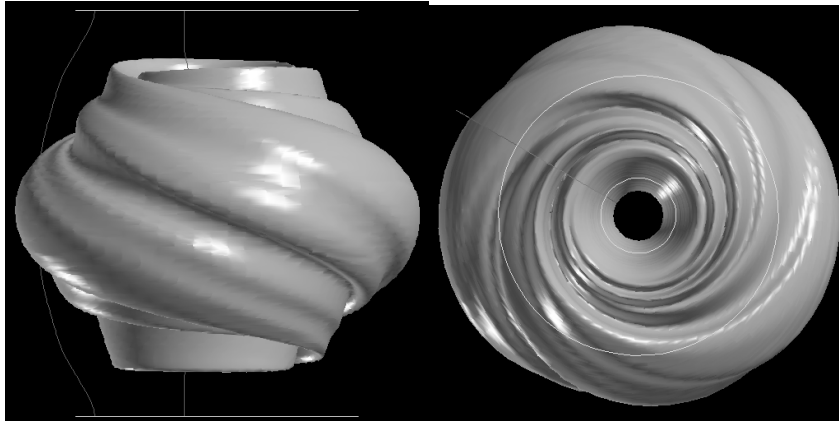


Fig. 5 Overall structure of the torus at $t=300$ (τ_A) shown by iso-surface of plasma pressure. The left panel is the side view, and the right panel is the top view.